Published in final edited form as:
Prog Biophys Mol Biol. 2012 October ; 110(2-3): 218–225. doi:10.1016/j.pbiomolbio.2012.07.010.

Mechanical Modulation of the Transverse Tubular System of Ventricular Cardiomyocytes

T. G. McNary[1,2,4], **K. W. Spitzer**[1], **H. Holloway**[3], **J. H. B. Bridge**[1], **P. Kohl**[4,5], and **F. B. Sachse**[1,2]

[1]Nora Eccles Harrison Cardiovascular Research and Training Institute, University of Utah, Salt Lake City, UT 84112, USA [2]Bioengineering Department, University of Utah, Salt Lake City, UT 84112, USA [3]Department of Anatomy with Radiology, University of Auckland, Park Road, Auckland, New Zealand [4]Department of Computing Science, University of Oxford, Parks Road, Oxford OX1 3QD, UK [5]National Heart and Lung Institute, Imperial College London, Harefield UB9 6JH, UK

Abstract

In most mammalian cardiomyocytes, the transverse tubular system (t-system) is a major site for electrical signaling and excitation-contraction coupling. T-tubules consist of membrane invaginations, which are decorated with various proteins involved in excitation-contraction coupling and mechano-electric feedback. Remodeling of the t-system has been reported for cells in culture and various types of heart disease. In this paper, we provide insights into effects of mechanical strain on the t-system in rabbit left ventricular myocytes. Based on fluorescent labeling, three-dimensional scanning confocal microscopy, and digital image analysis, we studied living and fixed isolated cells in different strain conditions. We extracted geometric features of t-tubules and characterized their arrangement with respect to the Z-disk. In addition, we studied the t-system in cells from hearts fixed either at zero left ventricular pressure (slack), at 30 mmHg (volume overload), or during lithium-induced contracture, using transmission electron microscopy. Two-dimensional image analysis was used to extract features of t-tubule cross-sections. Our analyses of confocal microscopic images showed that contracture at the cellular level causes deformation of the t-system, increasing the length and volume of t-tubules, and altering their cross-sectional shape. TEM data reconfirmed the presence of mechanically induced changes in T-tubular cross sections. In summary, our studies suggest that passive longitudinal stretching and active contraction of ventricular cardiomyocytes affect the geometry of t-tubules. This confirms that mechanical changes at cellular levels could promote alterations in partial volumes that would support a convection-assisted mode of exchange between the t-system content and extracellular space.

Corresponding Authors: Dr.-Ing. habil. Frank B. Sachse, University of Utah, Nora Eccles Harrison Cardiovascular Research and Training Institute, 95 South 2000 East, Salt Lake City, UT 84112-5000, USA, fs@cvrti.utah.edu, Phone: 801-587-9514, Fax: 801-581-3128, Dr. Thomas G. McNary, University of Utah, Nora Eccles Harrison Cardiovascular Research and Training Institute, 95 South 2000 East, Salt Lake City, UT 84112-5000, USA, mcnary@cvrti.utah.edu, Phone: 801-581-8183, Fax: 801-581-3128.

Keywords

transverse tubule; myocyte; strain; contraction; confocal microscopy

1. Introduction

The sarcolemma of ventricular and some atrial cardiomyocytes contains a characteristic system of invaginations called the transverse tubular system (t-system) (Dibb et al., 2009; Fawcett and McNutt, 1969; Simpson and Oertelis, 1962). These invaginations at sub-microscopic to microscopic scale are found in mammalian, but not in avian, reptile or amphibian cardiomyocytes (Bossen and Sommer, 1984; Bossen et al., 1978). Volume, diameter and length of t-tubules, and the morphology of the t-system as a whole, were found to depend on species and cell origin (Bers, 2001). In some species, these invaginations are primarily transversal, for instance, t-tubules in rabbit ventricular myocytes penetrate deep into the cell and are commonly unconnected (Savio-Galimberti et al., 2008). In other species, such as rat, the t-system includes connections that axially link t-tubules in ventricular myocytes, and this has been referred to as the transversal-axial tubular system (Asghari et al., 2009; Forbes et al., 1984; Soeller and Cannell, 1999).

The t-system plays important roles in trans-sarcolemmal electrical signaling. The lumina of t-tubules are continuous with the extracellular space. Thus, electrical signals from the outer sarcolemma can penetrate deep into the cell, which has been suggested to synchronize excitation-contraction coupling in ventricular cardiomyocytes (Brette and Orchard, 2003; Cordeiro et al., 2001). Calcium is the major signaling molecule in excitation-contraction coupling, and many proteins involved in calcium signaling are closely associated with the t-system (Asghari et al., 2009; Brette et al., 2006; Crossman et al., 2011), including L-type calcium channels (Brandt, 1985), Na^+/Ca^{2+} exchangers (Yang et al., 2002), and sarcolemmal Ca^{2+} ATPase pumps (Chase and Orchard, 2011). Inside the cell, the sarcoplasmic reticulum, which acts as the main store for calcium within cardiac myocytes, is closely associated with t-tubules (Iribe et al., 2009). Clusters of sarcoplasmic reticulum calcium release channels (ryanodine receptors, RyRs) exhibit a high density in close proximity to the t-system. Together, RyRs and L-type calcium channel comprise a basic structural and functional unit, the so-called couplon, which is thought to underlie calcium-induced calcium release in cardiac ventricular myocytes.

Various types of heart disease have been associated with a reduction in t-system density and topological disarrangement (Brette and Orchard, 2003; Ibrahim et al., 2011). For instance, remodeling of the t-system has been found in infarction-induced congestive heart failure in mouse (Louch et al., 2006), idiopathic dilated cardiomyopathy in human (Crossman et al., 2011) and dyssynchronous heart failure in canine (Sachse et al., 2012). Interestingly, mechanical unloading of the rat heart can also be accompanied by irregular distributions and reduced densities of t-tubules (Ibrahim et al., 2010). In fact, it may not be so much the absolute levels of tissue stress or strain, but their inhomogeneity, that gives rise to t-system disarray. Thus, a recent study (Sachse et al., 2012) showed that cardiac resynchronization therapy is associated with partial restoration of t-system organization after prior induction of dyssynchronous heart failure. Remodeling of the t-system in rat ventricular myocytes has also been reported for exercise-induced hypertrophy (Kemi et al., 2011), although in this setting, t-system density remains unchanged in spite of (physiological) hypertrophy of cardiomyocytes.

Several studies indicate functional consequences of t-system remodeling in heart disease, in particular for excitation-contraction coupling. Pathophysiological t-system remodeling has

been associated with reduced synchrony of calcium release as well as with reductions in the amplitude, upstroke velocity and decay dynamics of calcium transients (Louch et al., 2004; Lyon et al., 2009; Sachse et al., 2012). These functional consequences of t-system loss are probably a result of reduced association of RyRs with t-tubules and overall loss of t-system associated proteins (Brette and Orchard, 2003; Cordeiro et al., 2001; Yang et al., 2002).

While the t-system is crucial for coordinated contraction in mammalian ventricular myocytes, its mechanical and structural properties are not well characterized. For instance, mechanisms transferring mechanical strain from the cellular level to the t-system are not well understood. Various cytoskeletal proteins are present in the proximity of t-tubules, which could support strain transfer from the cell surface to the t-system (Kaprielian et al., 2000; Kostin et al., 1998). This transfer is believed to be important for mechanical signaling, for instance to non-selective stretch activated ion channels residing in the t-system (Sachs, 2005). In addition, we have shown that microtubular integrity is a prerequisite for the strain-induced increase in Ca^{2+} spark rate in rat isolated ventricular myocytes subjected to axial distension (Iribe et al., 2009), suggesting that not only sarcolemmal but also intra-cellular ion channels may be mechano-sensitive.

Strain at the cellular level is transmitted to the t-system. We found that this causes a change in t-tubular mouth configuration (Kohl et al., 2003), and observed a reduction in length and volume of t-tubules, as well as changes in their cross-sectional shape (McNary et al., 2011). Our data suggest that strains as small as 5% affect the shape of t-tubules. This supports our hypothesis that length changes, such as occur during the cycle of contraction and relaxation, may support a convection-assisted mechanisms that enhances what is typically assumed to be a diffusive exchange of t-tubular content with the extracellular space (Kohl et al., 2003).

Here, we extended this research to gain further insights into the effects of cellular contraction (i.e. negative strain) on the t-system. We tested the hypothesis that contraction also affects the t-system geometry using our previously developed confocal imaging approach on living myocytes, as well as transmission electron microscopy (TEM) on fixed cardiac tissue. Finally, we studied the relationship between t-tubules and the sarcomeric cytoskeletal protein α-actinin to explore whether strain-modulation of t-tubule geometry might be mediated via this component of the cytoskeleton.

2. Methods

All procedures involving animals were approved by the Animal Care and Use Committee of the University of Utah and complied with National Institutes of Health Guide for the Care and Use of Laboratory Animals 1996 and the UK Animals (Scientific Procedures) Act 1986 guidelines.

2.1 Confocal Imaging of Living Cardiomyocytes

2.1.1 Solutions—Zero calcium solution contained (in mM): 92.0 NaCl, 4.4 KCl, 5.0 $MgCl_2$, 1.0 $Na_2H_2PO_4$, 24.0 HEPES, 11.0 glucose, 20.0 taurine, 5.7 creatine, 5.0 sodium pyruvate, 12.5 NaOH. The enzyme solution consisted of the zero calcium solution with 0.2 mg/mL Collagenase P (Roche, Mannheim, Germany), 0.06 mg/mL protease Type XIV (Sigma, St. Louis, MO, USA), and a final concentration of 0.05 mM $CaCl_2$. The washout solution consisted of the zero calcium solution with 0.05 mM $CaCl_2$.

The modified Tyrode's solution was composed of: 126.0 NaCl, 4.4 KCl, 5.0 $MgCl_2$, 24.0 HEPES, 11.0 glucose, 12.9 NaOH, and 1.0 $CaCl_2$. The zero sodium solution was similar to the modified Tyrode's solution except, NaCl was replaced by an equimolar amount of N-methyl-D-glucamine, $CaCl_2$ was 2.0 mM, and the solution was titrated to pH 7.4 using HCl.

The contracture solution consisted of 10 mM caffeine added to the zero sodium solution. The phosphate buffer solution (PBS) solution was composed of: NaCl 137.0, KCl 2.6, KH_2PO_4 1.8, Na_2HPO_4 10.1, and titrated to a pH of 7.4.

2.1.2 Cell Isolation and Superfusion Chamber—The methods for isolating adult cardiac myocytes from rabbit heart were published previously (McNary et al., 2011). In short, New Zealand white rabbits were anesthetized and anti-coagulated by intravenous administration of pentobarbital and heparin. The hearts were perfused with zero calcium isolation solution, in preparation for perfusion with enzyme solution, and followed by perfusion with washout solution. After washout, left ventricular tissue was minced in washout solution, and gently shaken before filtering off the tissue debris.

All cells imaged in this study were initially inspected using the transmission mode of the microscope. We used only cells that had a rectangular appearance and well-defined striations, and did not spontaneously contract. All experiments were conducted within 8 h of cell isolation. Isolated ventricular cells were superfused at 2–4 mL/min (room temperature), nominally replacing experimental chamber volume every ~5 s. The glass bottom of the chamber was coated with laminin (Collaborative Research, Bedford, MA, USA) to improve cell adhesion.

2.1.3 Stretching and Induction of Steady-State Contracture in Myocytes—Longitudinal stretching of myocytes was performed as previously described (McNary et al., 2011). In short, we forged glass tools by pulling and sealing glass electrodes before bending the tips by 70–80°. Laminin was applied to these tools to increase binding to the myocyte. We used these tools, connected to micromanipulators, to apply passive stretch to the isolated myocytes during imaging. For induction of steady-state contractures, cells were initially superfused with the modified Tyrode's solution followed by the zero sodium solution for 2 min. Contractures were elicited by switching to the sodium-free contracture solution containing 10 mM caffeine, causing rapid release of Ca^{2+} from the sarcoplasmic reticulum under conditions of inhibited sodium-calcium exchange. Solution flow was stopped when the contracture stabilized.

2.1.4 In Vitro-Labeling of Isolated Cells, Imaging and Image Processing—Under conditions of no bath flow, a fluorescent dye conjugated to a membrane impermeable molecule (Dextran, Alexa Fluor 488; 10,000 MW, Anionic, Fixable, Invitrogen, Carlsbad, CA) was added (~250 μg, dissolved in 40μL PBS) via pipette to the solution. Dextran conjugates have been used before for studies of t-system in rat ventricular myocytes (Soeller and Cannell, 1999). Myocyte imaging was typically conducted within 10 min, during which perfusate flow was halted, to preserve fluorescent marker concentration. Imaging was performed on a Zeiss LSM 5 Duo microscope using an oil immersion 63× objective with a numerical aperture of 1.4. In previous work (Savio-Galimberti et al., 2008), we measured point spread functions of this imaging system, suggesting that its spatial resolution is 0.28, 0.28 and 0.83 μm in x-, y- and z-directions, respectively. We acquired image stacks with a voxel size of 0.1, 0.1 and 0.2 μm in the x, y, and z-directions, respectively. Raw images of segments from myocyte in contracture are shown in Figs. 1A–C. Image stacks were pre-processed, segmented, and analyzed as described previously (McNary et al., 2011). In short, an iterative Richardson-Lucy deconvolution algorithm was applied to the images using one of the above point spread functions, which had been extracted from images of fluorescent beads 100 nm in diameter (Molecular Probes, Eugene, OR; excitation wavelength 505, emission wave length 515 nm). Mask images of the myocyte segments were generated by region-growing and morphological operators (Gonzalez and Woods, 1992). T-tubules inside of the masked region were segmented using a region-growing algorithm; an example is shown in Fig. 1D. Only non-furcated t-tubules in the first 10 μm above the cover slip, having

a length of at least 1 μm, were selected for further analysis. A centerline was fit using a least-squares method (Fig. 1E). Mean intensities of orthogonal cross-sections along the centerline were determined. Based on these intensities, we performed corrections to the segmentation of t-tubule mouth regions before further analyses. We removed cross-sections from mouth regions with intensity larger than 4 times the mean intensity of t-tubules cross-sections in middle most areas of the centerline. The correction was performed iteratively, evaluating the most distal cross-section of the mouth region in each iteration. This procedure involved removal up to 2 optical sections (i.e. no more than 0.4 μm). After this correction, length and volume of each t-tubule were determined.

Cross-sectional area was calculated as volume of a cross-section divided by spacing of cross-sections along the centerline. Additionally, we characterized t-tubules by principal component analysis of the image moments of spherical regions, which were regularly spaced (~0.2 μm) along the t-tubule centerline. The principal component analysis yielded eigenvectors $\mathbf{e_1}$, $\mathbf{e_2}$, and $\mathbf{e_3}$ associated with eigenvalues λ_1, λ_2, and λ_3 (Gonzalez and Woods, 1992). Cross-sections were characterized by the 2nd and 3rd eigenvectors and eigenvalues (Fig. 1F). Ellipticity, ε, of a t-tubule cross-section was defined as:

$$\varepsilon = 1 - \sqrt{\lambda_3/\lambda_2}$$

Using this definition, a circular cross-section has an ellipticity of zero. Based on the principal component analysis we identified the orientation of the minor cross-section eigenvector $\mathbf{e_3}$ of the t-tubule cross-section (Fig. 1G) versus the myocyte long axis. The orientation angle α was zero when parallel with the myocyte long axis.

A potentially more intuitive definition of this angle α is based on considering the major axis of the t-tubule cross-section (eigenvector $\mathbf{e_2}$) relative to the orientation of the z-lines of the cardiac myocyte (approximately parallel to the 2nd eigenvector of the cell): if α=0, the major axis of t-tubular cross sections is parallel to the z-line.

2.2 Confocal Imaging of Fixed Cardiomyocytes

2.2.1 Fixation of Isolated Cells and Fluorescent Labeling—Cells were fixed in rest and contracture using a 2% paraformaldehyde solution in PBS, and labeled with wheat germ agglutinin (WGA) conjugated to Alexa 555 (Invitrogen, Carlsbad, CA). After treatment with 0.05% Triton-X-100 and washing, a blocking solution containing 10% normal goat serum was applied. Afterwards we labeled for sarcomeric α-actinin, which is a cytoskeletal protein associated with Z-disks. The primary antibody was raised in mouse (EA-53, Abcam, Cambridge, MA). The secondary antibody applied was goat anti mouse conjugated to Alexa 633 (Invitrogen, Carlsbad, CA).

2.2.2 Imaging and Image Processing of Fixed Cells—The membrane was imaged using a laser with a wavelength of 543 nm and a 560 nm long pass filter. A laser with a wavelength of 633 nm and a 650 nm long pass filter were applied for imaging the α-actinin. Image pre-processing was performed as described in section 2.1.4. We analyzed the spacing of structures along the cell long axis (y-direction) using three-dimensional Fourier transform. The analysis comprised maxima detection after quadratic interpolation in the Fourier spectrum.

2.3 TEM Imaging and Analyses

Cardiac ventricular tissue from New Zealand white rabbits were prepared for and imaged with TEM as described previously (Kohl et al., 2003). In short, isolated hearts were quickly

mounted to a Langendorff perfusion system for coronary perfusion with Krebs-Henseleit solution at 37° C. After washout, modifications of the Krebs-Henseleit solution were used to induce either cardioplegia or contracture. Cardioplegia and contracture were caused by elevating potassium concentration to 25 mM and substituting NaCl with LiCl, respectively. Hearts were then fixed within 2–4 min of reaching their target mechanical state by coronary perfusion with Karnovsky's paraformaldehyde–glutaraldehyde fixative (Karnovsky, 1965). Three different mechanical states were studied: rest, stretched, and contracture. The stretched state was produced using a fluid filled balloon in the left ventricle, inflated to a pressure of 30 mmHg. After perfusion with Karnovsky's fixative excised tissue samples were post fixed in buffered 1% osmium tetroxide, dehydrated through a graded series of ethanol and propylene oxide and embedded in Agar 100 resin (Agar Scientific, Stansted, UK). Ultra thin sections were cut on a Leica UCT ultramicrotome (Leica, Wetzlar, Germany), stained with uranyl acetate and lead citrate and imaged using an FEI Tecnai G2 Spirit TWIN electron microscope (FEI, Hillsboro, Oregon, USA).

Images had a dimension of 2,896 × 3,728 pixels. The image resolution ranged from 400 to 714 pixels/μm. In these images, we measured the mean sarcomere length (*SL*) and the mean length of the A-bands. Images with large SL heterogeneities were excluded from analysis. The ratio of A-band length to *SL* (*A-SL ratio*) was determined as an indicator of relative strain (an *A-SL ratio* near 1 is indicative of maximum shortening). In previous work this measure was suggested to be independent of the angle at which a slice is cut relative to the main cell axis (Bub et al., 2010). A least squares linear fit was used to describe the *A-SL ratio* as a function of SL:

$$A\text{-}SL\ ratio = a\ SL + b$$

with the parameters a and b describing the slope and intercept of the linear fit.

T-tubule cross-sections were manually segmented using the Matlab (version R2011b, Mathworks, Natick, MA) function "roipoly" in order to calculate their area, orientation of minor and major axes. Two-dimensional principal component analysis was applied to determine the ellipticity and orientation of the segmented t-tubule cross-sections. Fourier analysis was used to determine the orientation of the sarcomeres in each slice. For each t-tubule cross-section, the angle between its minor axis and the sarcomere orientation was determined. This angle is identical to the angle between z-line orientation and the major axis of t-tubule cross-sections.

2.4 Analyses and Statistics

In this work, we characterized mechanical deformations of cells by the one-dimensional engineering (or Cauchy) strain e:

$$e = \frac{l}{L} - 1$$

with the original length L and the length l after stretching or in contracture. Thus, cells that are not deformed ($l=L$) have a strain of 0%. Stretching ($l>L$) and contracture ($l<L$) leads to positive and negative strain, respectively.

All analyses were performed using Matlab (Mathworks). Statistical significance for measured changes in t-tubule geometric features was evaluated using one-way ANOVA and post-hoc unpaired t-tests using Tukey-Kramer correction. A value of $p<0.05$ was considered significant. Data are presented as mean±standard deviation.

3. Results

3.1 Confocal Imaging of Living Cardiomyocytes

We acquired three-dimensional image stacks from 142 living cells of 21 animals. Only 93 image stacks with high contrast between the t-system and the intracellular space, an insignificant number of vacuoles and without drift were analyzed. Examples for pre-processed image stacks of cells in rest, contracture and stretch are shown in Fig. 2. In these analyses, we included image stacks from resting and stretched cells that we had previously reported on (McNary et al., 2011).

Statistical analyses of t-tubules are presented in Fig. 3 and Table 1. T-tubules were categorized according to the type and level of strain applied, i.e., control (0±4%, SL=1.89±0.0756 μm), 8% stretch (8±4%), 16% stretch (16±4%), 8% contracture (−8±4%), or 16% contracture (−16±4%). We found a decrease of mean t-tubule length and volume with increasing strain. Cross-sectional area did not exhibit significant differences over the strain range. The mean ellipticity ε of t-tubule cross-sections at all strains was close to a value of 0.2. The orientation angle α of t-tubule cross-sections exhibited a biphasic relationship to strain. Increased (versus control) orientation angles α were found for both, 16% contracture and 16% stretch.

3.2 Confocal Imaging of Fixed Cardiomyocytes

We imaged 40 fixed cells labeled with WGA and α-actinin from 5 different animals using scanning three-dimensional confocal microscopy. Eight image stacks were not processed because of low signal-to-noise ratio, drift and significant numbers of vacuoles. Examples for raw and pre-processed image data are presented in Fig. 4. The α-actinin signal was found in sheets providing a marker for sarcomeric Z-disks. T-tubules were primarily visible in clefts of the α-actinin sheets.

The spacing only in the cell long axis was extracted for both types of image data using Fourier analysis. The spacing of α-actinin distributions in control cells was 1.75±0.09 μm (number of cells: 11), while the spacing of t-system was 1.75±0.11 μm. The α-actinin and t-system spacing of myocytes (number of cells: 21, animals: 4) exposed to the contracture protocol was 1.58±0.06 and 1.58±0.12 μm, respectively.

3.3 TEM Imaging of Cardiomyocytes

We segmented 328 t-tubule cross-sections from 104 TEM images. Fig. 5A–C shows representative images from each group. Cross-sections with an ellipticity larger than 0.96 were not used for further analysis. All images and their t-tubule cross-sections were grouped according to the *A-SL ratio* and the associated *SL* range. Statistical data on the analysis are listed in Table 2 and Fig. 5D–F. The cross-sectional area decreased from 0.11±0.05 μm^2 in control to 0.08±0.05 μm^2 in contracture while remaining unchanged versus stretch (0.10±0.06 μm^2) (Fig. 5D). The orientation angle α increased monotonically with increasing *SL* from contracture (36.1±25.6°) to the stretched state (46.4±25.7°) (Fig. 5E). Ellipticity was close to a value of 0.34 for all *SL* ranges (Fig. 5F).

4. Discussion

In the present study, we applied several imaging-based approaches to elucidate the effects of mechanical strain on the geometry of the t-system in cardiomyocytes. Fluorescent labeling, confocal imaging and image processing allowed us to analyze three-dimensional features of the t-system in living myocytes in contracture, rest, and stretched states. We applied similar image processing methods to fixed myocytes in rest and contracture to gain insights into the

spatial relationship between t-tubules and Z-disks. Furthermore, TEM images of cardiac tissue in contracture, rest, and stretch were analyzed to study the effects of strain on t-tubule cross-sections at a nanometer scale.

The present results revealed an increase in both volume and length of t-system during contracture. This is consistent with our previous findings showing a decrease in t-tubule volume and length when myocytes are stretched by 15% along their long axis (McNary et al., 2011). Our studies demonstrate that strain-t-tubule volume and strain-t-tubule length relationships are negative for all strains during a cardiac cycle. These findings are consistent with our hypothesis that strain at the cellular level could cause fluid exchange between the t-system and extracellular space (Kohl et al., 2003; McNary et al., 2011; Savio-Galimberti et al., 2008).

Previous work in toad skeletal muscle suggested that t-system geometry is not affected by strain (Launikonis and Stephenson, 2002). However, a limitation of this study was its two-dimensional imaging approach, which makes it difficult to consider strain effects on the length of t-tubules within a myocyte. Based on our three-dimensional image analysis, the strain modulation of t-tubule length appears to be the major source of volumetric change. Furthermore, our finding of strain-modulation of the area of t-tubule cross-sections from analysis of the TEM data appears to be inconsistent with this study.

The mechanisms causing the strain-modulation of t-tubule length remain unknown. Cell membrane can only extend 2–4% without rupturing unless there is available slack membrane (Hamill and Martinac, 2001). Thus, the process by which the t-tubules extend and shorten could be explained by reconfiguration of the curvature of the membrane around the mouth region of the tubule and of membrane of the t-tubule in the depth of the cell in an accordion like fashion. This may be aided by anchoring t-tubular membrane in the depth of the cell. Whether or not integration of caveolae into the t-tubular sarcolemma can be promoted by mechanical strain is an interesting question for future investigation.

The analyses of TEM images presented here are partly in agreement with the analyses of the three-dimensional confocal image stacks. Both analyses yielded an increased orientation angle α for contracture and stretch. Furthermore, both analyses showed that strain has only weak effects on ellipticity of cross-sections. Values of ellipticity were higher in the analysis of TEM images than in the analysis of confocal image stacks. While the TEM analysis indicated a significant increase of the area of t-tubule cross-sections for control versus contracture, the analysis based on confocal image stacks indicated that cross-sectional area is not affected by strain. A potential explanation for these differences is the higher spatial resolution of the TEM images, which allows for a more accurate description of small structures and the curvature their surfaces. However, an alternative explanation for these differences is the difficulty orienting two-dimensional TEM images in such a manner that they are orthogonal to the principal axis the t-tubules (Bub et al., 2010). Variability in the slicing angles affects the shape of the t-tubule cross-sections and features extracted from the cross-sections.

Our study on fixed cardiomyocytes labeled with WGA and α-actinin provided insights into the spatial relationship of the t-system and the sarcomeric cytoskeleton in ventricular myocytes of rabbit. Visual inspection and Fourier analysis revealed that major components of the t-systems are aligned with Z-disks at rest and in contracture. This indicates a concordant deformation of the two structures during a cardiac cycle. Together with our finding of a negative strain-t-tubule length relationship this suggests that t-tubules are anchored to Z-disks or adjacent structures.

Limitations

We discussed limitations of confocal microscopy and our approaches for analysis of image data previously (McNary et al., 2011). A major limitation is the spatial resolution of confocal microscopy, which can be quantified using point spread functions (Bolte and Cordelieres, 2006). The point spread function depends on the numerical aperture of the objective lens, wavelengths of excitation and emission light, pinhole size, and other optical properties of the imaging system. The point spread function describes the blurring of a point source by the imaging system. Blurring limits the quantification of t-tubule length, diameter, volume and cross-sectional area. We attenuated these errors by three-dimensional deconvolution of the confocal image data. Furthermore, we considered the limited resolution by our choice of experimental model, i.e. ventricular cells of rabbit. The t-system in these cells is topologically less complex and exhibits larger diameters than the t-system in ventricular cells of other small mammals like rat and mouse.

A limitation of our study is caused by the static conditions of our experimental preparations. These conditions are different to the dynamic setting in a beating heart. Accordingly, our analysis did not investigate viscoelastic properties of the t-system in the time scale of a heartbeat, and observations are not paired.

Furthermore, we have no information on local effects of strain along t-tubules. For example, our analyses did not discriminate between the mouth and internal regions of the t-system. As strain changes t-tubule mouth geometry, this may have affected length measurements. Thus, our study does not provide insights in potentially local deformation and heterogeneous fluid exchange along t-tubules into the depth of the myocyte. Future studies might use markers based on fluorescent labeling of proteins and geometrical definitions of the t-tubule mouth to discriminate between the outer sarcolemma and internal regions of the t-tubule. We were unable to identify possibly different strain transfer mechanisms that may contribute to observed changes during passive stretch and active contracture.

Our analyses were restricted to t-tubules of simple topology. We excluded longitudinal and topologically more complex components of the t-system. That said, t-tubules of simple topology appear to dominate the t-system in ventricular myocytes from rabbit. In other species, this is more complex, e.g. the transverse-axial tubular system in rat ventricular myocytes (Soeller and Cannell, 1999). Also, processing of the mouth region, although performed with the utmost diligence, involves a specific uncertainty factor. Thresholding in intensity profiles was applied to exclude the outermost cross-sections that cover the t-tubule mouth region, where very large intensities are recorded. Those cross-sections were considered to be outside of the cells' t-system. Processing affected up to 0.4 μm, which is similar to mean changes in t-tubular length changes observed in this study. If axial strain affected mouth region processing results, this could have indirect effects on processed data (although it is unlikely that this could explain the t-tubular length differences observed at extreme levels of positive and negative cell strain). Further studies are necessary to understand strain effects on more complex t-systems.

Another limitation of our approach is related to the necessity of using isolated myocytes for live-cell studies. We cannot exclude possible damage of the t-system occurring during and after cell isolation. Damage could be, in part, caused by a mismatch between physiological colloid-oncotic and osmotic pressures and those that are present in experimental solutions. Most of our solutions were slightly hyposmotic (~285 mOsm), but even in iso-osmotic solutions, cardiomyocytes have been shown to lose t-tubules after isolation (Pavlovic et al., 2010). We addressed this issue by limiting our cell imaging to 8 h after isolation. We did not observe appreciable depletion of t-system density during this time.

Acknowledgments

This work was supported by awards from the Nora Eccles Treadwell Foundation (to F. B. Sachse and J. H. B. Bridge), the British Heart Foundation (to P. Kohl) and the National Institutes of Health (R01HL094464 to F.B. Sachse; R37HL042873 to K. W. Spitzer).

Abbreviations

t-tubule	transverse tubule
t-system	transverse tubular system
RyRs	ryanodine receptors
TEM	transmission electron microscopy
PBS	phosphate buffer solution
SL	sarcomere length
WGA	wheat germ agglutinin

References

Asghari P, Schulson M, Scriven DR, Martens G, Moore ED. Axial tubules of rat ventricular myocytes form multiple junctions with the sarcoplasmic reticulum. Biophys J. 2009; 96:4651–4660. [PubMed: 19486687]

Bers, DM. Excitation-Contraction Coupling and Cardiac Contractile Force. The Netherlands: Springer; 2001. p. 452

Bolte S, Cordelieres FP. A guided tour into subcellular colocalization analysis in light microscopy. J Microsc. 2006; 224:213–232. [PubMed: 17210054]

Bossen EH, Sommer JR. Comparative stereology of the lizard and frog myocardium. Tissue Cell. 1984; 16:173–178. [PubMed: 6610956]

Bossen EH, Sommer JR, Waugh RA. Comparative stereology of the mouse and finch left ventricle. Tissue Cell. 1978; 10:773–784. [PubMed: 746545]

Brandt N. Identification of two populations of cardiac microsomes with nitrendipine receptors: correlation of the distribution of dihydropyridine receptors with organelle specific markers. Arch Biochem Biophys. 1985; 242:306–319. [PubMed: 2996434]

Brette F, Orchard C. T-tubule function in mammalian cardiac myocytes. Circ Res. 2003; 92:1182–1192. [PubMed: 12805236]

Brette F, Sallé L, Orchard C. Quantification of calcium entry at the t-tubules and surface membrane in rat ventricular myocytes. Biophys J. 2006; 90:381–389. [PubMed: 16214862]

Bub G, Camelliti P, Bollensdorff C, Stuckey DJ, Picton G, Burton RA, Clarke K, Kohl P. Measurement and analysis of sarcomere length in rat cardiomyocytes in situ and in vitro. Am J Physiol Heart Circ Physiol. 2010; 298:H1616–H1625. [PubMed: 20228259]

Chase A, Orchard CH. Ca efflux via the sarcolemmal Ca ATPase occurs only in the t-tubules of rat ventricular myocytes. J Mol Cell Cardiol. 2011; 50:187–193. [PubMed: 20971118]

Cordeiro JM, Spitzer KW, Giles WR, Ershler PE, Cannell MB, Bridge JH. Location of the initiation site of calcium transients and sparks in rabbit heart Purkinje cells. J Physiol. 2001; 531:301–314. [PubMed: 11310434]

Crossman DJ, Ruygrok PR, Soeller C, Cannell MB. Changes in the organization of excitation-contraction coupling structures in failing human heart. PLoS One. 2011; 6:e17901. [PubMed: 21408028]

Dibb KM, Clarke JD, Horn MA, Richards MA, Graham HK, Eisner DA, Trafford AW. Characterization of an extensive transverse tubular network in sheep atrial myocytes and its depletion in heart failure. Circ Heart Fail. 2009; 2:482–489. [PubMed: 19808379]

Fawcett DW, McNutt NS. The ultrastructure of the cat myocardium. I. Ventricular papillary muscle. J Cell Biol. 1969; 42:1–45. [PubMed: 4891913]

Forbes MS, Hawkey LA, Sperelakis N. The transverse-axial tubular system (TATS) of mouse myocardium: its morphology in the developing and adult animal. Am J Anat. 1984; 170:143–162. [PubMed: 6465048]

Gonzalez, RC.; Woods, RE. Digital Image Processing, Addison-Wesley, Reading, MA. 1992.

Hamill OP, Martinac B. Molecular basis of mechanotransduction in living cells. Physiol Rev. 2001; 81:685–740. [PubMed: 11274342]

Ibrahim M, Al Masri A, Navaratnarajah M, Siedlecka U, Soppa GK, Moshkov A, Al-Saud SA, Gorelik J, Yacoub MH, Terracciano CM. Prolonged mechanical unloading affects cardiomyocyte excitation-contraction coupling, transverse-tubule structure, and the cell surface. FASEB J. 2010; 24:3321–3329. [PubMed: 20430793]

Ibrahim M, Gorelik J, Yacoub MH, Terracciano CM. The structure and function of cardiac t-tubules in health and disease. Proc Biol Sci. 2011; 278:2714–2723. [PubMed: 21697171]

Iribe G, Ward CW, Camelliti P, Bollensdorff C, Mason F, Burton RA, Garny A, Morphew MK, Hoenger A, Lederer WJ, Kohl P. Axial stretch of rat single ventricular cardiomyocytes causes an acute and transient increase in Ca2+ spark rate. Circ Res. 2009; 104:787–795. [PubMed: 19197074]

Kaprielian RR, Stevenson S, Rothery SM, Cullen MJ, Severs NJ. Distinct patterns of dystrophin organization in myocyte sarcolemma and transverse tubules of normal and diseased human myocardium. Circulation. 2000; 101:2586–2594. [PubMed: 10840009]

Karnovsky M. A formaldehyde-glutaraldehyde fixative of high osmolality for use in electron microscopy. J. Cell Biol. 1965; 27:137–138A.

Kemi OJ, Hoydal MA, Macquaide N, Haram PM, Koch LG, Britton SL, Ellingsen O, Smith GL, Wisloff U. The effect of exercise training on transverse tubules in normal, remodeled, and reverse remodeled hearts. J Cell Physiol. 2011; 226:2235–2243. [PubMed: 21660947]

Kohl P, Cooper PJ, Holloway H. Effects of acute ventricular volume manipulation on in situ cardiomyocyte cell membrane configuration. Prog Biophys Mol Biol. 2003; 82:221–227. [PubMed: 12732281]

Kostin S, Scholz D, Shimada T, Maeno Y, Mollnau H, Hein S, Schaper J. The internal and external protein scaffold of the T-tubular system in cardiomyocytes. Cell Tissue Res. 1998; 294:449–460. [PubMed: 9799462]

Launikonis BS, Stephenson DG. Tubular system volume changes in twitch fibres from toad and rat skeletal muscle assessed by confocal microscopy. J Physiol. 2002; 538:607–618. [PubMed: 11790823]

Louch WE, Bito V, Heinzel FR, Macianskiene R, Vanhaecke J, Flameng W, Mubagwa K, Sipido KR. Reduced synchrony of Ca2+ release with loss of T-tubules-a comparison to Ca2+ release in human failing cardiomyocytes. Cardiovasc Res. 2004; 62:63–73. [PubMed: 15023553]

Louch WE, Mork HK, Sexton J, Stromme TA, Laake P, Sjaastad I, Sejersted OM. T-tubule disorganization and reduced synchrony of Ca2+ release in murine cardiomyocytes following myocardial infarction. J Physiol. 2006; 574:519–533. [PubMed: 16709642]

Lyon AR, MacLeod KT, Zhang Y, Garcia E, Kanda GK, Lab MJ, Korchev YE, Harding SE, Gorelik J. Loss of T-tubules and other changes to surface topography in ventricular myocytes from failing human and rat heart. Proc Natl Acad Sci U S A. 2009; 106:6854–6859. [PubMed: 19342485]

McNary TG, Bridge JHB, Sachse FB. Strain transfer in ventricular cardiomyocytes to their transverse tubular system revealed by scanning confocal microscopy. Biophys J. 2011; 100:L01–L03.

Pavlovic D, McLatchie LM, Shattock MJ. The rate of loss of T-tubules in cultured adult ventricular myocytes is species dependent. Exp Physiol. 2010; 95:518–527. [PubMed: 20061354]

Sachs, F. Stretched activated channels in the heart. In: Kohl, P.; Sachs, F.; Franz, MR., editors. Cardiac mechano-electric feedback and arrythmias from pipette to patient. Elsevier Saunders; 2005. p. 2-9.

Sachse FB, Torres NS, Savio-Galimberti E, Aiba T, Kass DA, Tomaselli GF, Bridge JH. Subcellular Structures and Function of Myocytes Impaired During Heart Failure Are Restored by Cardiac Resynchronization Therapy. Circ Res. 2012

Savio-Galimberti E, Frank J, Inoue M, Goldhaber JI, Cannell MB, Bridge JH, Sachse FB. Novel features of the rabbit transverse tubular system revealed by quantitative analysis of three-dimensional reconstructions from confocal images. Biophys J. 2008; 95:2053–2062. [PubMed: 18487298]

Simpson FO, Oertelis SJ. The fine structure of sheep myocardial cells; sarcolemmal invaginations and the transverse tubular system. J Cell Biol. 1962; 12:91–100. [PubMed: 13913207]

Soeller C, Cannell MB. Examination of the transverse tubular system in living cardiac rat myocytes by 2-photon microscopy and digital image-processing techniques. Circ Res. 1999; 84:266–275. [PubMed: 10024300]

Yang Z, Pascarel C, Steele DS, Komukai K, Brette F, Orchard CH. Na+-Ca2+ exchange activity is localized in the T-tubules of rat ventricular myocytes. Circ Res. 2002; 91:315–322. [PubMed: 12193464]

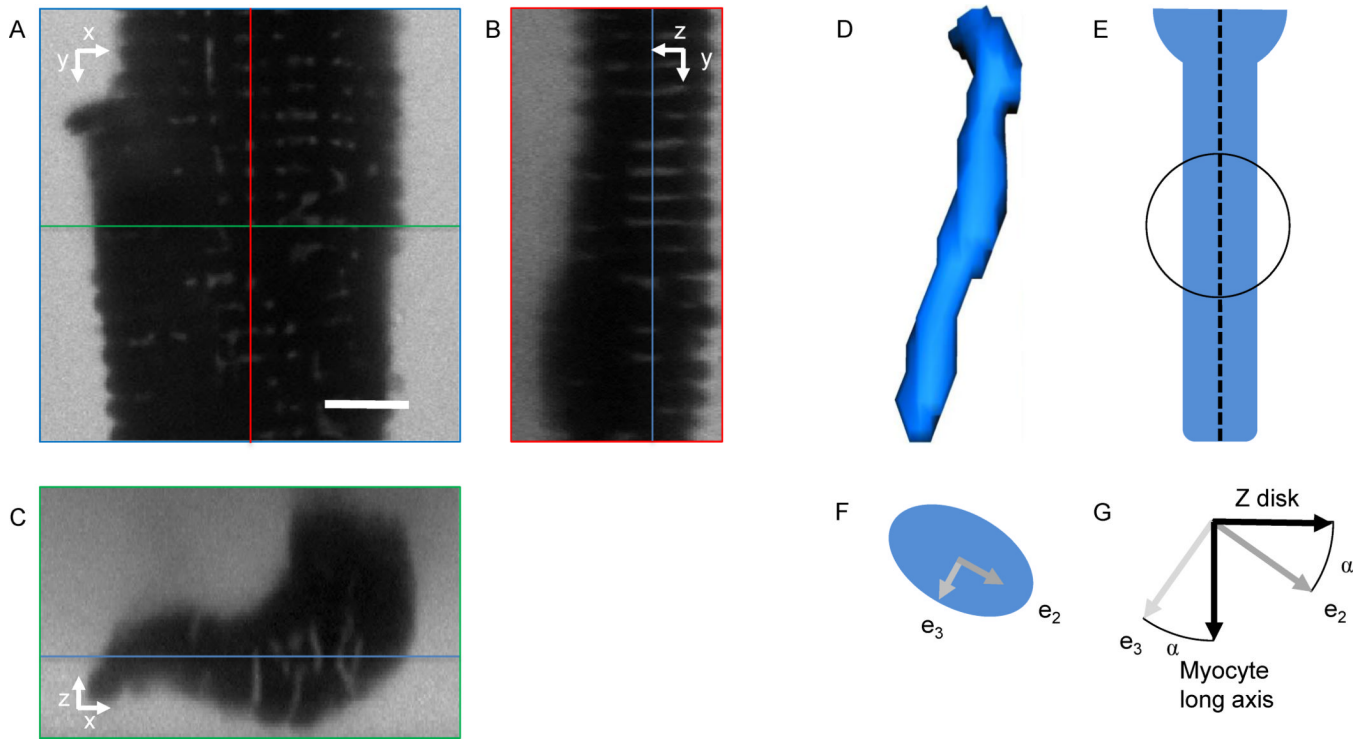

Figure 1.

Imaging of myocytes and geometrical characterization of t-tubules. A segment of a myocyte in contracture was imaged using confocal microscopy and cross-section are presented along the (A) x- and y-, (B) y- and z-, and (C) x- and z-axes. Red, green and blue lines specify positions of the cross-sections presented in (B), (C) and (A), respectively. (D) T-tubules were segmented by region-growing. (E) After fitting of a centerline (dashed), spherical regions along the centerline were analyzed using principal component analysis. (F) T-tubule cross-sections in spherical regions were described by the eigenvectors e_2 and e_3. (G) Orientation of t-tubule cross-sections was measured as the angle α between the minor cross-section eigenvector e_3 and the myocyte long axis (1st eigenvector of the cell). Assuming that z-disks are perpendicular to the long axis of the myocyte, the same angle α can be measured between the cross-section eigenvector e_2 and the z-disks (2nd and 3rd eigenvector of the cell). Scale bar: 5 μm.

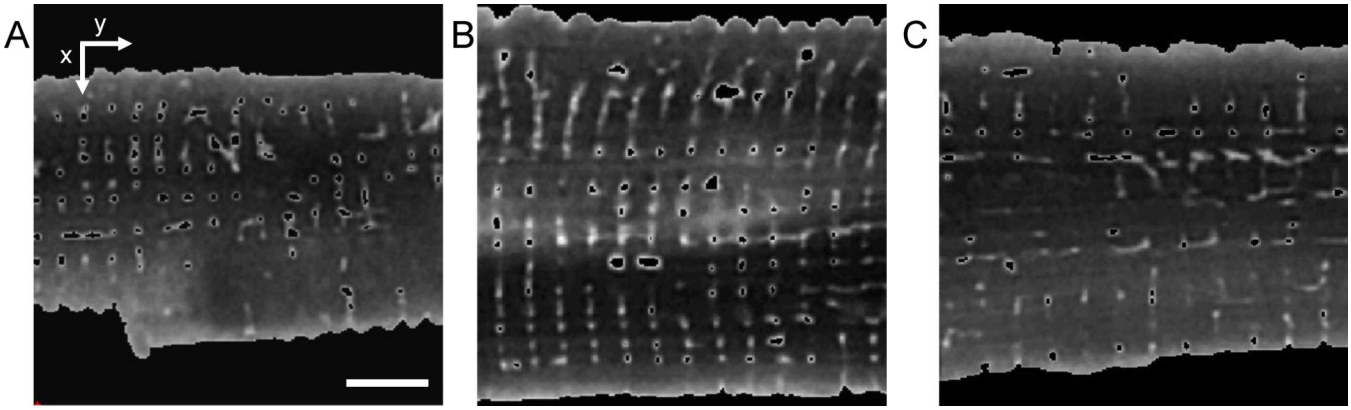

Figure 2.

Cross-sections from processed image stack of a myocyte in (A) contracture, (B) rest, and (C) after stretching. The *SL* of the cells in (A), (B) and (C) is 1.60, 1.90 and 2.18 μm, respectively. Masks were applied to each image stack to label the cell inside including t-system. The t-tubules were segmented using the region growing method. Scale bar: 5 μm.

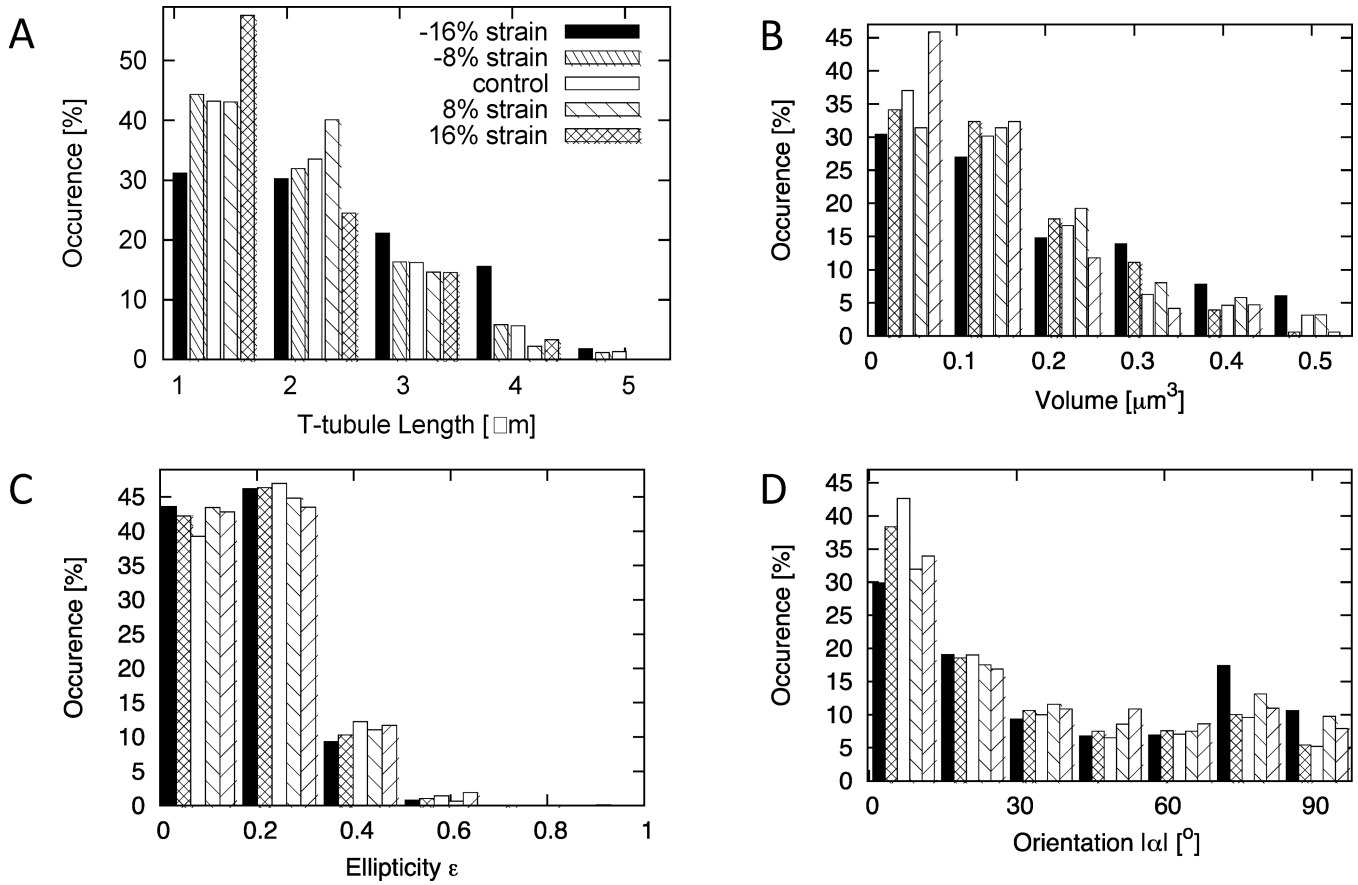

Figure 3.

Statistical analysis of t-tubules segmented in three-dimensional image stacks. Histograms of (A) t-tubule length, (B) volume, (C) ellipticity and (D) orientation of crosssections are presented during contraction, control, and strain. A *SL* of 1.89 μm was identified with 0% strain. Each category spanned a strain range of ±4%.

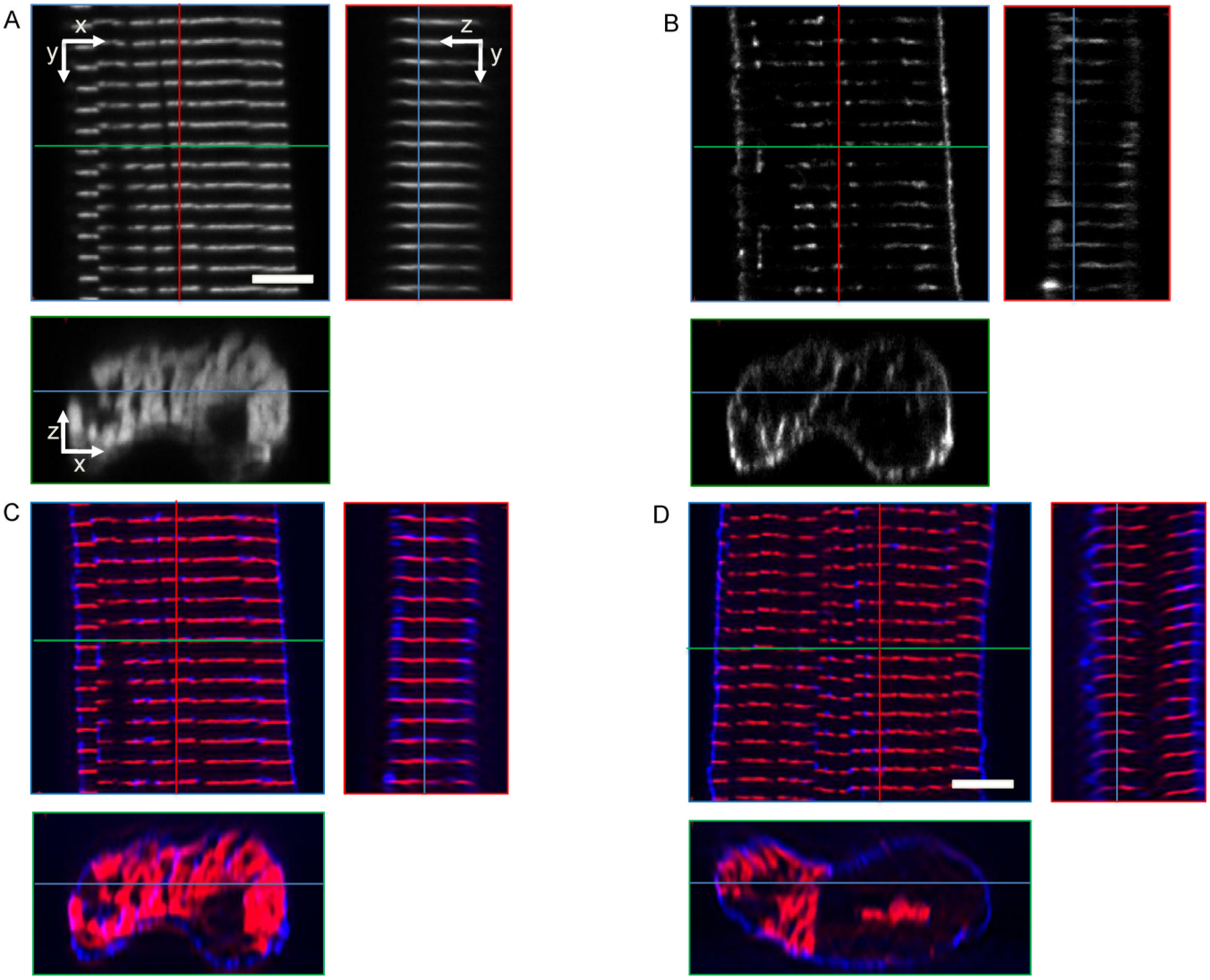

Figure 4.

Cross-sections from image stacks of segments of fixed cells. A cell in rest labeled with (A) α-actinin and (B) WGA was imaged using confocal microscopy. (C) The overlay of images presented in (A) and (B) illustrates the spatial relationship of sarcolemma and t-system (blue) to α-actinin (red). (D) Images from a cell in contracture. Red, green and blue lines indicate positions of yz, xz and xy cross-sections, respectively. Scale bars: 5 μm.

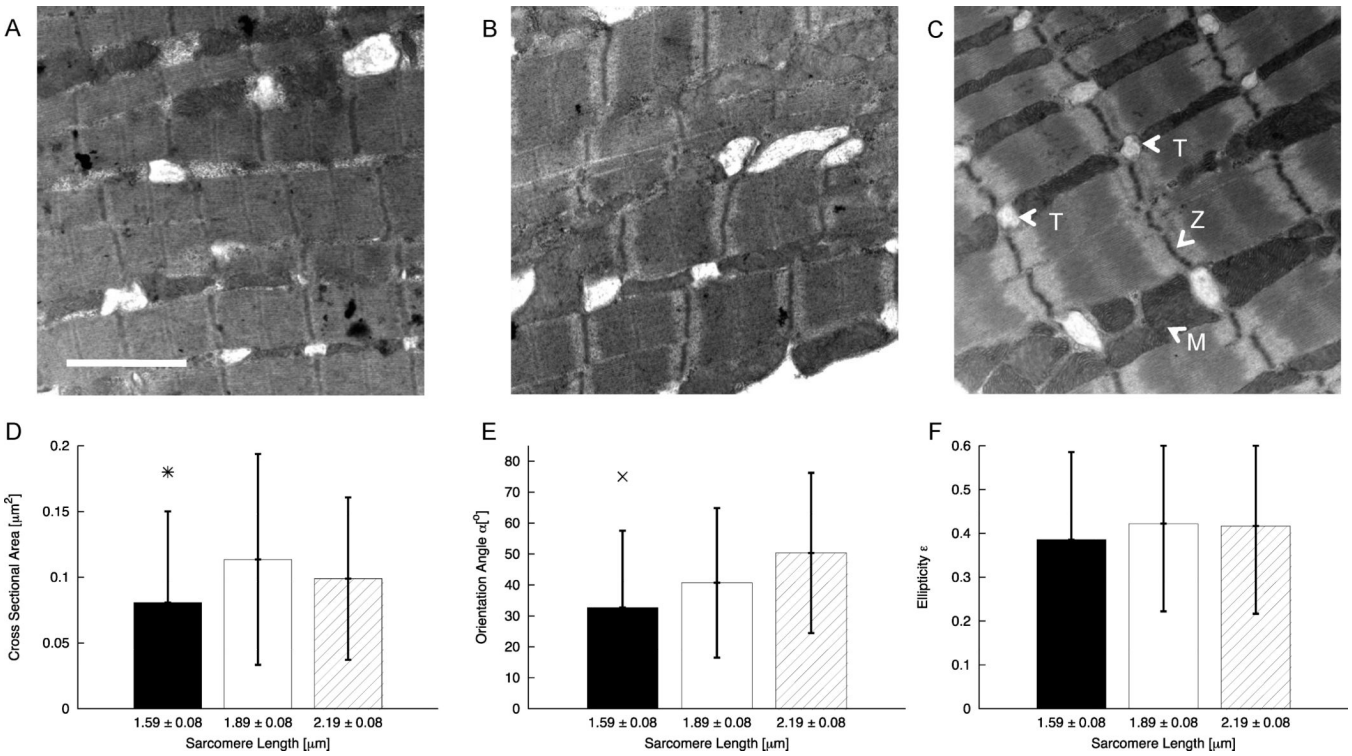

Figure 5.

TEM images and statistical analyses of TEM images from cardiac tissue in (A) contracture, (B) rest, and (C) stretched. In (C), some t-tubules (T), Z-lines (Z), and mitochondria (M) are marked. (D) The t-tubule cross-sectional area in cells in contracture is reduced versus cells in rest. (E) The orientation angle α of t-tubule cross-sections is increased in stretched cells versus cells in contracture. (F) Ellipticity of cross-sections was not affected by strain. Bars show standard deviation. *significant difference of contracture *vs.* rest; [x] significant difference contracture *vs.* stretched. Scale bar: 2 μm.

Table 1

Statistical analyses of t-tubules from confocal microscopic images of living cells.

	−16% Strain	**−8% Strain**	**Control**	**8% Strain**	**16% Strain**
Number of animals	3	6	15	9	9
Number of t-tubules	109	257	997	196	151
Number of cross-sections	1252	2567	9995	1843	1311
Length [μm]	2.42±0.97 *†	2.14±0.88	2.08±0.86	1.97±0.71	1.86±0.76 *
Volume [μm^3]	0.22±0.14 *†	0.18±0.12	0.18±0.13	0.18±0.12	0.16±0.11 *
Cross-sectional area [μm^2]	0.084±0.032	0.080±0.032	0.079±0.031	0.083±0.0394	0.078±0.029
Ellipticity ε	0.19±0.11 *†	0.20±0.10 †	0.20±0.11	0.19±0.10 †*	0.20±0.11
Orientation |α|[°]	39.2±30.7 *†	30.7±27.6	29.9±27.7	34.4± 29.2 *	33.8±28.2 *

*Significant *vs.* control.

†Significant *vs.* 16% strain.

Table 2

Statistical data on TEM image analysis.

	Contracture	Control	Stretch
Number of animals	2	2	2
Number of cross-sections	47	69	82
SL [μm]	1.69±0.10	1.96±0.07	2.21±0.11
A-SL ratio	0.898±0.012	0.778±0.014	0.697±0.019